Quantitative Analysis of Nonuniform Distributions in Lung Perfusion Scintigraphy

Osamu Mitomo, Sakae Aoki, Takeshi Tsunoda, Masafumi Yamaguchi and Hidemasa Kuwabara

Departments of Radiology and Internal Medicine, National Numata Hospital, Gunma Prefecture, Japan

Nonuniform distributions of lung perfusion scintiscans obtained by SPECT were quantified to supplement qualitative lung scintiscans. A total of 126 lung perfusion scintigraphy examinations were performed between February and December 1996 on a subject population of 102 patients, including 8 control subjects. All of the subjects were broadly classified according to whether they had pulmonary disease or nonpulmonary disease. The latter group was subdivided into a group with cardiac disease and other diseases. The grade of breathlessness was classified according to whether oxygen inhalation was required, the clinical severity of the breathlessness and patient's performance status. Blood gas analysis was performed in 21 cases, and pulmonary function testing was performed in 26 cases. **Methods:** With the subjects resting in the supine position, 185 MBq ^{99m}Tc-macroaggregate albumin was infused. From reconstructed SPECT images, the volume of lung as a whole calculated at 10% of threshold was assumed to be the functional lung volume, and the functional volume rates were calculated in 10% threshold widths from 10% to 100% of thresholds. Assuming the total absolute difference in functional volume rate between each subject and the control to be the distribution index of the lung as a whole (D index), we quantified the degree of nonuniform distribution in each subject. **Results:** The D index of all subjects ranged from 2.7 to 72.2. The mean D index in pulmonary disease was significantly higher than in nonpulmonary disease (p < 0.0005) and cardiac disease (p < 0.005). It was significantly positively correlated with the grade of breathlessness, significantly negatively correlated with the oxygenation index and significantly positively correlated with measured vital capacity and forced expiratory volume in 1 sec as percentages of their predicted values. **Conclusion:** The D index is a useful indicator for quantifying nonuniform distributions on lung scintiscans. If it is used as a supplement to qualitative interpretation of scintiscans, pulmonary perfusion scintigraphy will become a more useful technique for clinical evaluation of treatment and assessment of breathlessness and respiratory failure than the usual one.

Key Words: lung perfusion; SPECT; nonuniform distribution; quantification of nonuniform distribution

J Nucl Med 1998; 39:1630–1635

Lung perfusion scintigraphy is a familiar and convenient nuclear medicine technique that has often been used qualitatively and visually, especially to diagnose abnormal pulmonary arterial blood flow or abnormal ventilation (1–4).

To enhance the characteristics of lung perfusion scintigraphy and to supplement qualitative diagnosis, nonuniform distributions on lung perfusion scintiscans by SPECT were quantified.

MATERIALS AND METHODS

A total of 126 lung perfusion scintiscans were performed in National Numata Hospital between February and December 1996, excluding cases of superior vena cava syndrome, and the subject population consisted of 102 patients, including 8 control subjects with no complaints of breathlessness or chest pain and no abnormal findings on chest radiographs and CT examinations (Table 1). The age range was 39–89 yr, and the mean age was 69.6 yr. All subjects were broadly classified according to whether they had pulmonary or nonpulmonary disease. The former included chronic obstructive lung disease, inflammatory disease, primary lung cancer, pulmonary infarction and pulmonary hypertension. The latter was divided into two subgroups: a cardiac group, which included myocardial infarction, hypertrophic cardiomyopathy and valvular disease, and another disease group, which included malignancies other than primary lung cancer, diffuse liver disease and complaints of general malaise.

The grade of breathlessness was classified according to whether oxygen inhalation was required, the clinical classification of breathlessness (Table 2) and performance status (Table 3). In 21 cases, blood gas analysis was performed at rest within 3 days of the lung scintigraphy. In 26 cases, pulmonary function testing was performed within 2 wk of the lung scintigraphy. The interval between pulmonary function testing and scintigraphy was 4.9 ± 4.6 days (mean ± s.d.).

After the subjects had rested sufficiently in the supine position, 185 MBq ^{99m}Tc-macroaggregate albumin (MAA, Lungscinti ^{99m}Tc injectable; Nihon Medi-Physics Co., Nishinomiya, Japan) was infused into an antecubital vein with the patient's arm elevated.

The gamma camera was a two-detector rotating system (MULTISPECT 2; Siemens Medical Systems, Hoffman Estates, IL). High-resolution collimators were used, and zoom size was 1.45. A 20% window width was centered on the ^{99m}Tc photopeak (140 keV). Pairs of projection images were recorded for 25 sec at 5° intervals over 180°, and a total of 72 projections were acquired. Each projection had a matrix size of 128 × 128. The data were reconstructed by filtered backprojection using a fifth-order Butterworth filter with a cutoff frequency of 0.23 cycles/pixel. There was no attenuation correction. Tomographic sections 9.93 mm thick with a pixel size of 3.31 mm were generated in the transverse, sagittal and coronal planes. The window level limits ranged from 0% to 100%.

The volume calculated from the SPECT images at the 10% cutoff threshold was assumed to be the functional lung volume of the lung (V). The functional lung volumes of the lung as a whole ranged from 1886 ml to 5887 ml (mean ± s.d.: 3767 ± 905 ml). The distribution index of the lung as a whole, the D index, was calculated as shown in Table 4:

$$D = \int_{n=1}^{n=9} |r_n - r_n^c| \times 100.$$

The threshold width number (n) was taken from 1 to 9 for every additional 10% threshold. For example, letting t be threshold (%), threshold number is 1 for $10 \leq t < 20$, 2 for $20 \leq t < 30 \ldots 9$ for $90 \leq t \leq 100$, successively. The functional volume rate (r_n) was calculated as the functional volume (v_n) divided by the functional lung volume of the lung (V). The functional volume (v_n) and functional volume rate (r_n) were calculated for threshold width number separately. V^c, v_n^c and r_n^c were the mean of functional lung

TABLE 1
Classification of Patient Population According to Disease

Disease	No. of cases	Total no.	No. of men/ no. of women	Age (yr)
Pulmonary	65	87	67/20	70.5 ± 8.9
Nonpulmonary	29	31 (9)	15/16 (2/7)	66.9 ± 13.4 (71.9 ± 13.1)
Total	94	118	82/36	69.6 ± 10.4

Numbers in parentheses are values for cardiac disease; values are means ± s.d.

volume of the lung, the functional volume and the functional volume rate of the eight control subjects, respectively.

The functional volume rate curves of the lung as a whole in the eight control subjects are shown in Figure 1.

Comparisons between groups were performed using the unpaired Student's t-test, with $p < 0.05$ taken to represent significance. Correlation coefficients were calculated by linear regression analysis. A value of $p < 0.05$ was considered to be significant.

RESULTS

The D index in the subjects as a whole ranged from 2.7 to 72.2 (mean ± s.d.: 23.7 ± 14.7). The mean D index in pulmonary disease was significantly higher than in nonpulmo-

TABLE 2
Classification of Breathlessness

Severity	Respiratory symptoms
I (normal)	Able to walk on the level or go up stairs the same as healthy persons of the same age.
II (mild)	Able to walk on the level, but cannot go up stairs or inclines the same as healthy persons of the same age.
III (moderate)	Able to walk more than 1 km at one's own pace but cannot walk as fast as healthy persons of the same age.
IV (severe)	Unable to walk more than 50 m without taking a short rest.
V (very severe)	Occurrence of breathlessness while talking, taking off one's clothes or looking after oneself.

TABLE 3
Grade of Breathlessness

	Grade		
	Mild	Moderate	Severe
Oxygen inhalation	(−)	(−)	(+)
Classification of breathlessness	I–II	III	IV–V
Performance status	0–1	2	3–4
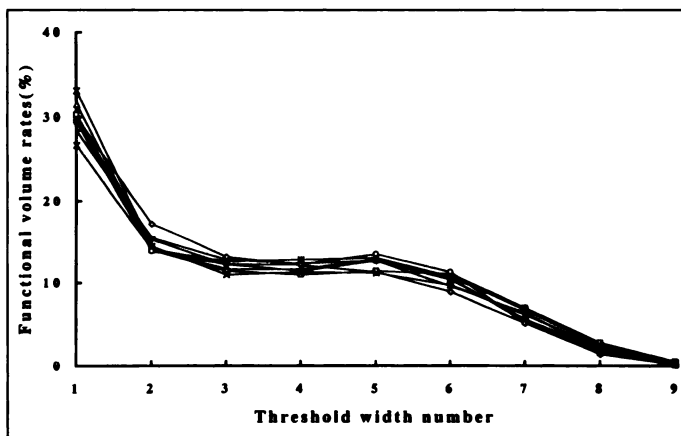
FIGURE 1. Functional volume rate curves in eight control subjects.

nary disease and significantly higher than in cardiac disease and other diseases (Table 5). The D index significantly increased as the grade of breathlessness became more severe (Table 6). The D index was significantly negatively correlated with the oxygenation index (PaO_2-to-FiO_2 ratio) (Fig. 2). The D index was significantly positively correlated with measured vital capacity as a percentage of the predicted value (%VC) and measured forced expiratory volume in 1 sec as a percentage of observed forced expiratory 1-sec volume by predicted value ($FEV_{1.0}$%) (Fig. 3).

CASE REPORTS

The functional volume rate curves of patients who complained of mild and severe breathlessness and a control curve are reported (Fig. 4). The findings in a lung cancer patient (Fig. 5) demonstrate improvement in the D index after radiotherapy for a right lower lobe lung tumor.

DISCUSSION

Lung perfusion scintigraphy has provided visual representations (2–7) and quantitative predictions of pulmonary function after surgery and radiotherapy (6) (8–11). In addition, lung SPECT has also been used for quantitative evaluation of pulmonary function (12–14).

SPECT has facilitated three-dimensional evaluation of the degree of nonuniform distribution itself, but there have been no reports of quantitative analysis to evaluate nonuniform distribution in the lung. Although it is important to evaluate the segments that are impaired, we have often found that it is necessary to quantitatively evaluate the degree of nonuniform distribution itself, especially when diagnosing the severity or extent of diffuse impaired pulmonary vessels in diffuse lung disease. The interpretation of whether or not scintiscans are uniform and what degree of nonuniform distributions they are tend to be subjective and may vary according to the conditions

TABLE 4
Procedure Used to Calculate Distribution Index

Threshold (t)	$10 \le t < 20$	$20 \le t < 30$	—	$80 \le t < 90$	$90 \le t$	Summation
Threshold width number (n)	1	2	—	8	9	
Functional volume (v_n)	v_1	v_2	—	v_8	v_9	$\Sigma_1^9 v_n = V$
Functional volume rate (r_n)	r_1	Y_2	—	r_8	r_9	$\Sigma_1^9 r_n = 1$
Functional volume of control (v_n^c)	v_1^c	v_2^c	—	v_8^c	v_9^c	$\Sigma_1^9 v_n^c = V^c$
Functional volume rate of control (r_n^c)	r_1^c	r_2^c	—	r_8^c	r_9^c	$\Sigma_1^9 r_n^c = 1$
Absolute differences between r_n and r_n^c	$\|r_1 - r_1^c\|$	$\|r_2 - r_2^c\|$	—	$\|r_8 - r_8^c\|$	$\|r_9 - r_9^c\|$	D/100

$r_n = v_n/V$, $r_n^c = v_n^c/V^c$; v_n^c, r_n^c and V^c are mean of eight control subjects.

TABLE 5
Distribution Index of Diseases

Disease	No. of subjects	Distribution index
Pulmonary	87	26.5 ± 15.1*†‡
Nonpulmonary	31	15.9 ± 10.0*
Cardiac	9	11.7 ± 4.5†
Other	22	17.6 ± 11.2‡
Total	118	23.7 ± 14.7

*p < 0.0004.
†p < 0.005.
‡p = 0.011.
Values are means ± s.d.

under which the scintiscans were obtained. A quantitative analysis of the degree of the nonuniformity of the distributions by using three-dimensional reconstruction of the lung SPECT as a mean of objective interpretation of scintiscans was attempted.

A large majority of ^{99m}Tc-MAA particles infused into the peripheral vein are impacted in the lungs. Generally, extrapulmonary accumulation of ^{99m}Tc-MAA is unusual in routine lung scanning (15–19). Although Arroyo et al. (20) reported that gallbladder activity in lung perfusion studies was a fairly common finding, the gallbladder was never visualized in our studies.

The lung distribution of ^{99m}Tc-MAA may not be completely uniform even in normal subjects. Lisbona et al. (21) suggested that lung perfusion in normal subjects at rest is inherently nonuniform. The cause of the nonuniformity of distribution had chiefly been ascribed to gravity (22–25), but Glenny et al. (26) suggested that gravitation plays a secondary role in the heterogeneity of distribution. They stated that the major determinant of perfusion heterogeneity is a complex and dynamic structure
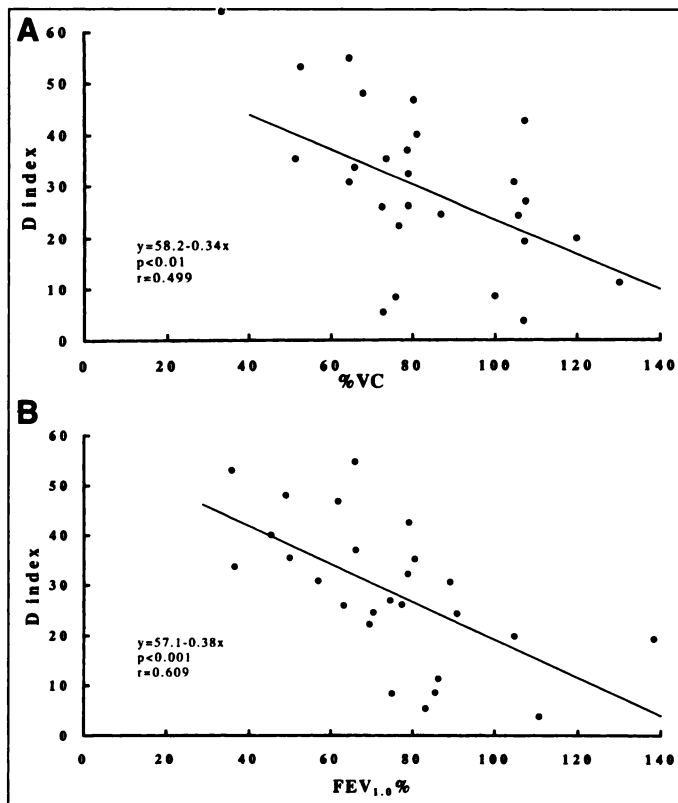
TABLE 6
Distribution Index of the Grade of Breathlessness

Grade of breathlessness	No. of subjects	Distribution index
Mild	58	16.2 ± 9.8*‡
Moderate	21	25.4 ± 11.9*†
Severe	39	33.8 ± 16.0‡†

*p < 0.001.
†p < 0.038.
‡p = 0.0001.
Values are means ± s.d.
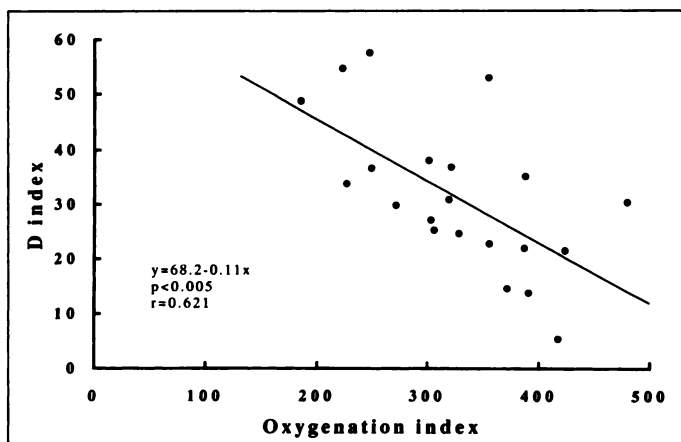
**FIGURE 2.** Oxygenation and distribution indices.

FIGURE 3. (A) Correlation between measured vital capacity as a percentage of the predicted value (%VC) and distribution (D) index. (B) Correlation between measured forced expiratory volume in 1 sec as a percentage of the predicted value (FEV$_{1.0}$%) and D index.

and that this is a constant factor independent of posture and time. As Wiener et al. (27) indicated about the ventilation, the organs surrounding the lung may also affect the distribution of perfusion. Various factors, for example, gravity, lung structure, organs surrounding the lung and other as yet unidentified factors that might be responsible, resulted in the inherently nonuniform distributions in normal subjects.

The functional lung volumes reconstructed from the SPECT images vary depending on the threshold values that have been preset. The three-dimensional volume reconstructed at the 10% threshold was assumed to be the functional lung volume (V) for each subject and calculated functional volume (v_n) and volume rate (r_n) for each of the nine threshold width numbers for the lung as a whole (Table 4). The functional volume rate curves of the eight controls showed similar patterns (Fig. 1). The inherently nonuniform distributions in normal subjects resulted in these patterns, and we used the averaged functional volume rate curve of the controls as the standard curve to quantify the degree of nonuniformity of distribution in perfusion scintiscans of the subjects. As damage to pulmonary vessels increases, the volume and volume rate of decreased accumulation of MAA and the impairment of pulmonary flow ultimately result in a shift of the functional volume rate curve from the standard curve. Figure 4 shows that the more nonuniform the distributions are, the further the functional volume rate curve shifts above or below the standard curve. Assuming that the absolute differences between the standard curve and the shifted functional volume rate curve of the subjects correlate with the degree of nonuniformity of distribution, as quantitative indicators of distribution we calculated the D index for the lung as a whole.

The D index was significantly positively correlated with the presence of pulmonary disease and the grade of breathlessness
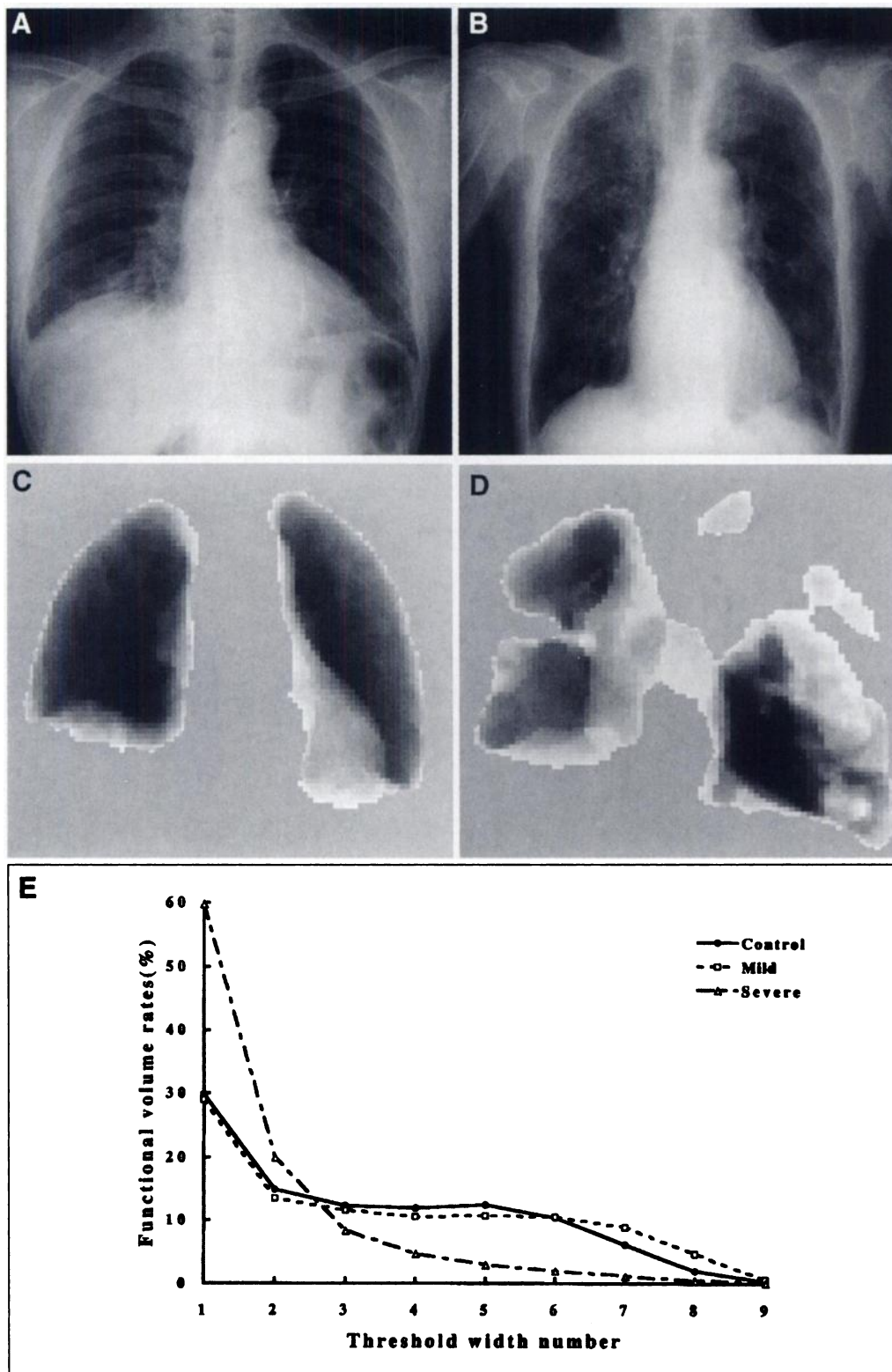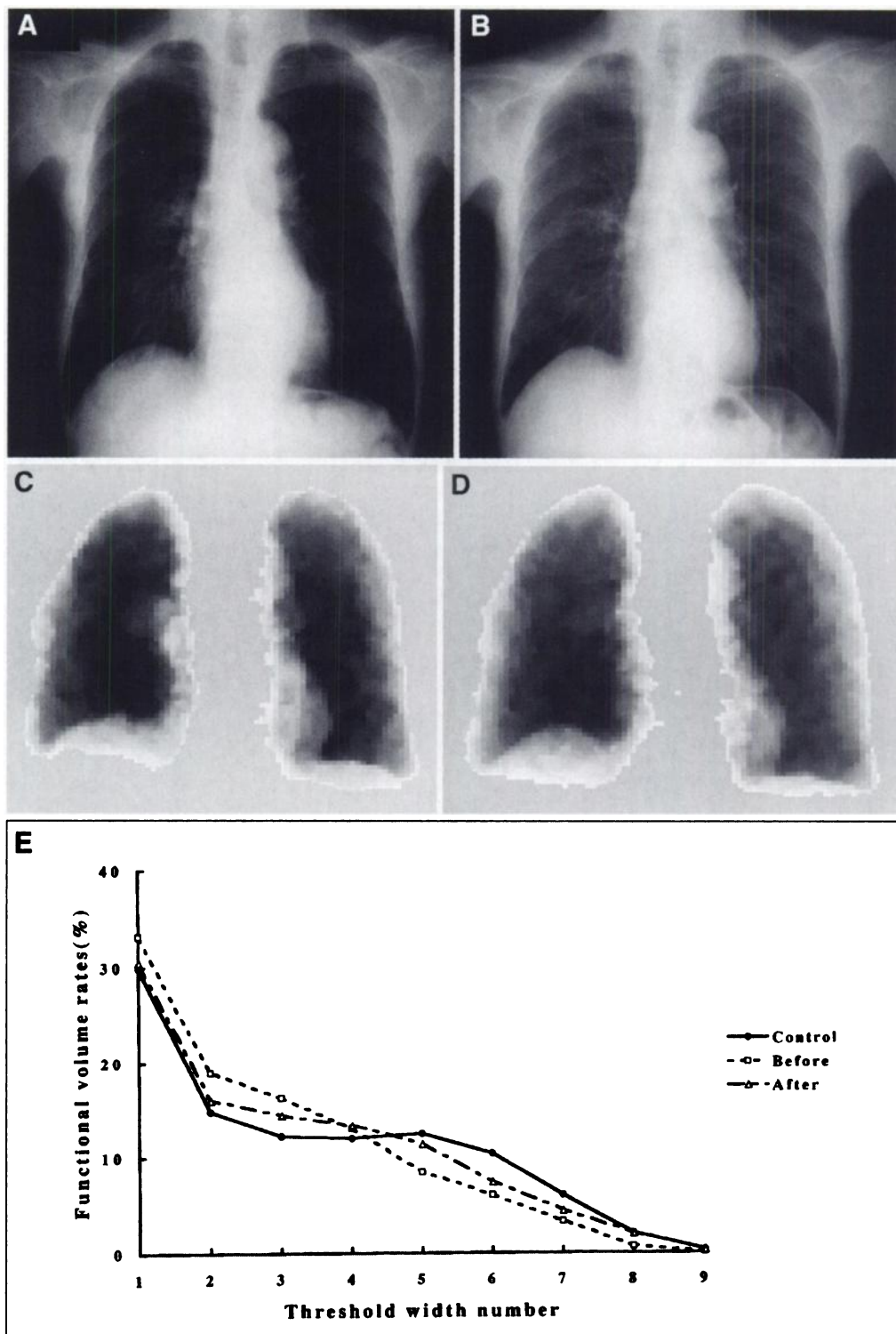
FIGURE 4. Chest radiographs (A and B) and three-dimensional functional lung volume images (C and D) of mild and severe cases of breathlessness, respectively. (E) Functional volume rate curves of lung as a whole of control and mild and severe cases of breathlessness. The control curve is the averaged functional volume rate curve of eight control subjects. Distribution indices in mild and severe cases were 12 and 70.3, respectively.

but significantly negatively correlated with the oxygenation index of arterial blood and pulmonary function test values (%VC, $FEV_{1.0}$%). Generally, it is considered that the pulmonary disease, grade of breathlessness and decrease of oxygenation index of arterial blood and pulmonary function test values relate with the impairment of the pulmonary arteries to a greater or lesser degree, resulting in nonuniform distributions of the pulmonary scintigraphy through the reconstruction or remodeling of intrapulmonary blood flows. And so it is thought that these results show that quantitative analysis of nonuniform

distribution of the lung as a whole, the D index, may be a useful indicator for evaluating the impairments of the intrapulmonary blood flows.

The mean D index in clinically diagnosed cardiac disease was significantly lower than in pulmonary disease. The D index will be able to provide useful information to quantitatively judge which cardiac or pulmonary factor is the main cause of breathlessness. When the nine cases of cardiac disease were excluded, the mean D indices for mild, moderate and severe breathlessness were 16.3, 26.3 and 37.9, respectively. There

FIGURE 5. Chest radiographs (A and B) and three-dimensional functional lung volume images (C and D) before and after conventional radiotherapy, respectively. (E) Volume rate curves before and after conventional radiotherapy. The distribution index decreased from 25.4 to 12.2, and the improvement of nonuniform distribution was shown. About each lung of right and left lungs, the functional volumes, the functional volume rates and the distribution indices (D_r and D_l index) were calculated in the same manner according to Table 4. D_r and D_l indices also decreased from 12.5 to 6.5 and from 15.7 to 8.3, respectively, before and after radiotherapy.

were more significant correlations between the D index and the grade of breathlessness. As an objective index of grade of breathlessness, which is a subjective determination, a D index of below 10, 10–20, 20–30 and above 30 grossly corresponds to normal, mild, moderate and severe breathlessness, respectively.

This study is a clinical attempt to quantify the nonuniformity of lung scintiscans. The D index was worked out by going a step further in the process of calculations of functional lung volumes and reconstructions of three-dimensional lung images using the SPECT technique. If this analysis is used as supplement to qualitative and visual interpretation of planar, SPECT and reconstructed three-dimensional lung images, lung perfusion scintigraphy using the D index will become a more useful

technique for clinical evaluation of medical treatment of various lung diseases and for quantitative measurement of breathlessness and respiratory failure than usual ones.

CONCLUSION

To supplement qualitative lung scintiscans, the D index was obtained as the indicator of nonuniform distribution to quantify the nonuniform distributions of lung perfusion scintiscans by SPECT. A total of 126 lung perfusion scintigraphy examinations were performed from February and December 1996 on a subject population of 102 patients, including the 8 control subjects. The D index is a useful indicator for quantifying nonuniform distributions on lung scintiscans. If it is used as a

supplement to qualitative interpretation of scintiscans, pulmonary perfusion scintigraphy will become a more useful technique for clinical evaluation of treatment and assessment of breathlessness and respiratory failure than the usual one.

REFERENCES

1. Wagner HN Jr, Sabiston DC Jr, McAee JG, Tow D, Stern HS. Diagnosis of massive pulmonary embolism in man by radioisotope scanning. *N Engl J Med* 1964;271:377–384.
2. Maynard CD, Cowan RJ. Role of the scan in bronchogenic carcinoma. *Semin Nucl Med* 1971;1:195–205.
3. Newman GE, Sullivan DC, Gottschalk A, Putman CE. Scintigraphic perfusion patterns in patients with diffuse lung disease. *Radiology* 1982;143:227–231.
4. Clarke SEM, Secker-Walker RH. Lung scanning. In: Maisey MN, Britton KE, Gilday DL, eds. *Clinical nuclear medicine*, 2nd ed. London: Chapman and Hall Medical; 1991:47–74.
5. Garnett ES, Goddard BA, Fraser HS, Macleod WM. Lung perfusion patterns in carcinoma of bronchus. *Br Med J* 1968;2:209–210.
6. Macumber HH, Calvin JW. Perfusion lung scan patterns in 100 patients with bronchogenic carcinoma. *J Thorac Cardiovasc Surg* 1976;72:299–302.
7. Frankel N, Coleman RE, Pryor DB, Sostman HD, Ravin CE. Utilization of lung scans by clinicians. *J Nucl Med* 1986;27:366–369.
8. Olsen GN, Block AJ, Tobias JA. Prediction of postpneumonectomy pulmonary function using quantitative macroaggregate lung scanning. *Chest* 1974;66:13–16.
9. Fazio F, Pratt TA, McKenzie CG, Steiner RE. Improvement in regional ventilation and perfusion after radiotherapy for unresectable carcinoma of the bronchus. *Am J Roentgenol* 1979;133:191–200.
10. Rubenstein JH, Richter MP, Moldofsky PJ, Solin LJ. Prospective prediction of post-radiation therapy lung function using quantitative lung scan and pulmonary function testing. *Int J Radiat Oncol Biol Phys* 1988;15:83–87.
11. Moldofsky PJ, Rubenstein JH, Richter MP, Solin LJ, Gatenby RA, Broder GJ. Quantitative lung scans for prediction of post-radiotherapy pulmonary function. *Clin Nucl Med* 1988;13:644–646.
12. Touya JJ, Corbus HF, Savala KM, Habibe MN. Single photon emission computed tomography in the diagnosis of pulmonary thromboembolism. *Semin Nucl Med* 1986;16:306–336.
13. Hirose Y, Imaeda T, Doi H, Kokubo M, Sakai S, Hirose H. Lung perfusion SPECT in predicting postoperative pulmonary function in lung cancer. *Ann Nucl Med* 1993;7:123–126.
14. Hosokawa N, Tanabe M, Satoh K, et al. Prediction of postoperative pulmonary function using ^{99m}Tc-MAA perfusion lung SPECT. *Nippon Acta Radiol* 1995;55:414–422.
15. Richards-Carty C, Mishkin FS. Hepatic activity on perfusion lung images. *Semin Nucl Med* 1987;17:85–86.
16. Kitani K, Taplin GV. Biliary excretion of ^{99m}Tc-albumin microaggregate degradation products (a method for measuring Kupffer cell digestive function?). *J Nucl Med* 1972;13:260–265.
17. Marcus CS, Parker LS, Rose JG, Cullison RC, Grady PJ. Uptake of ^{99m}Tc-MAA by the liver during a thromboscintigram/lung scan. *J Nucl Med* 1983;24:36–38.
18. Gates GF, Goris ML. Suitability of radiopharmaceuticals for determining right-to-left shunting: concise communication. *J Nucl Med* 1977;18:255–257.
19. Dlabal PW, Stutts BS, Lenkins DW, Harkleroad LE, Stanford WT. Cyanosis following right pneumonectomy: importance of patent foramen ovale. *Chest* 1982;81:370–372.
20. Arroyo AJ, Jenkins TJ, Patel YP. Gallbladder visualization on routine lung perfusion imaging. *Clin Nucl Med* 1997;22:42–45.
21. Lisbona R, Dean GW, Hakim TS. Observations with SPECT on the normal regional distribution of pulmonary blood flow in gravity independent planes. *J Nucl Med* 1987;28:1758–1762.
22. Permutt S, Bromberger-Barnea B, Bane HN. Alveolar pressure, pulmonary venous pressure, and the vascular waterfall. *Med Thorac* 1962;19:239–260.
23. Anthonisen NR, Milic-Emili J. Distribution of pulmonary perfusion in erect man. *J Appl Physiol* 1966;21:760–766.
24. Hughes JMB, Glazier JB, Maloney JE, West JB. Effect of lung volume on the distribution of pulmonary blood flow in man. *Respir Physiol* 1968;4:58–72.
25. Maeda H, Itoh H, Ishii Y, et al. Pulmonary blood flow distribution measured by radionuclide-computed tomography. *J Appl Physiol* 1985;54:225–233.
26. Glenny RW, Polissar L, Robertson HT. Relative contribution of gravity to pulmonary perfusion heterogeneity. *J Appl Physiol* 1991;71:2449–2452.
27. Wiener CM, Mckenna WJ, Myers MJ, Lavender JP, Hughes JMB. Left lower lobe ventilation is reduced in patients with cardiomegaly in the supine but not the prone position. *Am Rev Respir Dis* 1990;141:150–155.

Lymphoscintigraphy and Lymphangiography of Lymphangiectasia

Douglas Howarth and Peter Gloviczki
Department of Nuclear Medicine, John Hunter Hospital, Newcastle, Australia; and Division of Vascular Surgery, Mayo Clinic, Rochester, Minnesota

Chronic genital edema secondary to lymphangiectasia and chylous reflux in a 23-yr-old man with Noonan syndrome was investigated by ^{99m}Tc sulfur nanocolloid lymphoscintigraphy and bipedal contrast lymphangiography. Lymphoscintigraphy showed a delayed lymphatic flow pattern in the pelvis, abdomen and chest consistent with lymphangiectasia and abnormal lymphatic flow dynamics. Lymphangiography showed dilated and tortuous abnormal lymphatics in the abdomen and pelvis. Ligation of incompetent retroperitoneal lymph vessels and lymphaticovenous anastamosis were performed, resulting in clinical improvement. Lymphangiectasia has been described previously in Noonan syndrome, but it is relatively uncommon below the diaphragm. This case demonstrates the use of lymphoscintigraphy and lymphangiography in providing important physiological and anatomical information before surgical intervention. Careful presurgical planning using such tests also allows the most appropriate operation to be performed.

Key Words: Noonan syndrome; lymphangiectasia; lymphoscintigraphy; lymphangiography

Noonan syndrome is characterized by wide-ranging phenotypic features, many of which are also seen in Turner's

syndrome (*1,2*). The more common congenital cardiovascular abnormalities include pulmonary valvular stenosis, hypertrophic cardiomyopathy and atrial septal defect; however, abnormalities of the lymphatic system are also well recognized (*3–7*). In some patients, peripheral lymphoscintigraphy may be helpful in distinguishing primary lymphedema from secondary lymphedema and further evaluating congenital lymphatic abnormalities (*8*). Peripheral lymphoscintigraphy demonstrates normal or abnormal lymphatic transport of radiolabeled nanocolloid in patterns that may be diagnostic, but it more often provides additional information confirming or refuting the clinical diagnosis. Accurate anatomical detail is not, however, provided by lymphoscintigraphy and, under some circumstances, when lymphatic surgery is planned lymphangiography may also be helpful. We describe a patient with retroperitoneal lymphangiectasia in whom lymphoscintigraphy and lymphangiography were complementary in planning lymphatic surgery.

CASE REPORT

A 23-yr-old man with a sporadic form of Noonan syndrome characterized by slightly wide-spaced eyes and low-set ears, mild pectus excavatum, previous surgically corrected right cryptorchidism and moderate pulmonary stenosis/regurgitation presented with a 7-yr history of genital edema and chronic painless eruption of scrotal vesicles associated with fluid